



# Flagellin engineering enhances CAR-T cell function by reshaping tumor microenvironment in solid tumors

Xiangyun Niu <sup>1,2</sup> Pengchao Zhang,<sup>1,2</sup> Liujiang Dai,<sup>1</sup> Xixia Peng,<sup>1</sup> Zhongming Liu,<sup>1</sup> Yexiao Tang,<sup>1</sup> Guizhong Zhang <sup>1</sup> Xiaochun Wan<sup>1</sup>

**To cite:** Niu X, Zhang P, Dai L, *et al.* Flagellin engineering enhances CAR-T cell function by reshaping tumor microenvironment in solid tumors. *Journal for ImmunoTherapy of Cancer* 2025;**13**:e010237. doi:10.1136/jitc-2024-010237

► Additional supplemental material is published online only. To view, please visit the journal online (<https://doi.org/10.1136/jitc-2024-010237>).

Accepted 21 March 2025



© Author(s) (or their employer(s)) 2025. Re-use permitted under CC BY-NC. No commercial re-use. See rights and permissions. Published by BMJ Group.

<sup>1</sup>Shenzhen Institutes of Advanced Technology Chinese Academy of Sciences, Shenzhen, Guangdong, China  
<sup>2</sup>University of Chinese Academy of Sciences, Beijing, China

**Correspondence to**  
Dr Guizhong Zhang;  
gz.zhang@siat.ac.cn

Dr Xiaochun Wan;  
xc.wan@siat.ac.cn

## ABSTRACT

**Background** Adoptive cell therapy using genetically engineered chimeric antigen receptor (CAR)-T cells is a new type of immunotherapy that directs T cells to target cancer specifically. Although CAR-T therapy has achieved significant clinical efficacy in treating hematologic malignancies, its therapeutic benefit in solid tumors is impeded by the immunosuppressive tumor microenvironment (TME). Therefore, we sought to remodel the TME by activating tumor-infiltrating immune cells to enhance the antitumor function of CAR-T cells.

**Methods** We engineered CAR-T cells expressing *Salmonella* flagellin (Fla), a ligand for toll-like receptor 5, to activate immune cells and reshape the TME in solid tumors. Functional validation of the novel Fla-engineered CAR-T cells was performed in co-cultures and mouse tumor models.

**Results** Fla could activate tumor-associated macrophages and dendritic cells, reshaping the TME to establish an “immune-hot” milieu. Notably, this “cold” to “hot” evolution not only improved CAR-T cell function for better control of target-positive tumors, but also encouraged the production of endogenous cytotoxic CD8<sup>+</sup>T cells, which targeted more tumor-associated antigens and were thus more effective against tumors with antigenic heterogeneity.

**Conclusion** Our study reveals the potential and cellular mechanisms for Fla to rewire antitumor immunity. It also implies that modifying CAR-T cells to express Fla is a viable strategy to improve the efficacy of CAR-T cell treatment against solid tumors.

## BACKGROUND

Adoptive cellular therapy using chimeric antigen receptor (CAR)-T cells has shown remarkable therapeutic outcomes in hematologic malignancies.<sup>1</sup> However, the application of CAR-T cell therapy in solid tumors has fallen short of anticipated efficacy. Challenges such as tumor antigenic heterogeneity, immunosuppressive tumor microenvironment (TME), and T-cell exhaustion within solid tumors, significantly diminish the therapeutic effects.<sup>2</sup> Various cell types within the TME contribute to immune suppression, including myeloid-derived suppressor cells

## WHAT IS ALREADY KNOWN ON THIS TOPIC

⇒ The therapeutic benefits of chimeric antigen receptor (CAR)-T cells in solid tumors are severely impeded by the immunosuppressive tumor microenvironment (TME).

## WHAT THIS STUDY ADDS

⇒ Delivering flagellin into tumors via CAR-T cells can remodel the TME by activating tumor-associated macrophages and dendritic cells, which enhances the therapeutic effects of CAR-T cells and also encourages endogenous CD8<sup>+</sup>T cell-mediated antitumor responses in solid tumors.

## HOW THIS STUDY MIGHT AFFECT RESEARCH, PRACTICE OR POLICY

⇒ This study introduces an innovative strategy to enhance the efficacy of CAR-T cells by incorporating an additional immune-stimulating pathway. This approach holds substantial translational potential, as it can be applied to various solid tumors with immunosuppressive TME.

(MDSCs), tumor-associated macrophages (TAMs) and regulatory T cells (Tregs), which express immunosuppressive molecules, thereby compromising the function of infiltrating CAR-T cells.<sup>3</sup> Therefore, equipping CAR-T cells with the potential to induce TME remodeling is critical to improve the efficacy of CAR-T cell treatment for solid tumors.

Several strategies, including arming CAR-T cells with immune-stimulating signals, can enhance their efficacy and activate endogenous antitumor responses by reshaping the TME of solid tumors.<sup>4–6</sup> Flagellin (Fla) is the structural protein subunit found in the bacterial flagellum, a locomotory organ commonly associated with gram-negative bacteria. Toll-like receptor 5 (TLR5) specifically recognizes Fla and is expressed on various innate immune cells, including monocytes, macrophages, and dendritic cells (DCs).<sup>7</sup> TLR5 binds to monomeric Fla, triggering an intracellular signaling cascade that activates

numerous proinflammatory genes. Due to its potent immunostimulatory properties, Fla is widely used as a vaccine adjuvant.<sup>8–10</sup> Recently, Fla has been demonstrated to impede tumor growth by directly binding to TLR5<sup>+</sup> tumor cells and inhibiting their proliferation.<sup>11</sup> It can also stimulate and mobilize immune cells to create antitumor immune responses.<sup>9, 12, 13</sup> Fla may therefore have potent antitumor effects either on its own or in conjunction with immunotherapy. Intratumoral constitutive delivery of Fla as a payload for T cells has been shown to significantly enhance the efficacy of tumor immunotherapy, without inducing notable systemic toxicity during experimental observation.<sup>14</sup> However, this continuous delivery approach lacks a built-in regulatory or termination mechanism, posing potential risks from prolonged Fla leakage, even after the tumor has been cleared by T cells in vivo. SynNotch CAR-T cells offer a promising platform for localized delivery of various therapeutic agents, including Fla.<sup>15</sup> Despite this potential, in vivo efficacy has yet to be demonstrated. Additionally, even with successful delivery, the CAR signal does not trigger T cell cytotoxicity, hindering the realization of potential synergistic effects between CAR-T cells and Fla. As a result, there is currently no reliable and safe method for combining CAR-T cells with Fla, and the therapeutic potential of this combination has yet to undergo systematic evaluation.

Here we found that CAR-T cells engineered to secrete Fla under the control of natural CAR signaling, rather than synNotch CAR signaling, enable the specific delivery of Fla. This approach could overcome the immunosuppressive TME and antigenic heterogeneity by activating endogenous tumor-infiltrating immune cells, thereby enhancing the antitumor activity of CAR-T cells in solid tumors. Our study provides a novel strategy to incorporate immune-stimulating signaling to adoptively transferred tumor-specific T cells within the TME, thereby improving their efficacy.

## METHODS

### Cell lines

B16F10, MC38, HCT116, and HEK293T cells were cultured in Dulbecco's Modified Eagle Medium (DMEM) with 10% fetal bovine serum (FBS, Gibco), 100 U/mL penicillin, and 100 µg/mL streptomycin. To generate antigen-positive cell lines, B16F10 and MC38 cells were transduced with lentiviral vectors encoding truncated murine or human CD19, firefly luciferase, and puromycin N-acetyltransferase (pLV-mCD19t-P2A-fLuc-T2A-puro or pLV-hCD19t-P2A-fLuc-T2A-puro) and selected with 7.5 µg/mL puromycin (Beyotime); HCT116 cells were transduced with pLV-hCD19t-P2A-fLuc-T2A-puro and selected with 1 µg/mL puromycin. CD19 expression was evaluated by flow cytometry (CytoFLEX, Beckman Coulter) using Alexa Fluor 700-conjugated anti-mouse CD19 (BioLegend, clone: 6D5) and APC-conjugated anti-human CD19 antibodies (BioLegend, clone: HIB19). To generate firefly luciferase-expressing control cells,

B16F10 cells were transduced with pLV-fLuc-T2A-puro and selected with 7.5 µg/mL puromycin.

### Cloning and constructs

To generate CAR vectors for murine CAR-T cell preparation, the CAR sequence targeting murine CD19 (mCD19)<sup>16</sup> with an single chain fragment variable (scFv) domain (derived from 1D3), CD28 transmembrane domain, CD28 costimulatory signal, and CD3ζ domain was synthesized and cloned into MIGR1 (pRV-mCD19CAR). A flag tag was inserted between the signal peptide and scFv domain for CAR expression detection. The codon-optimized Fla sequence (derived from *Salmonella fliC*) was fused with an N-terminal mouse IgGκ signal peptide and a C-terminal 6×His tag, inserted downstream of a 4×Nuclear factor of activated T cells (NFAT)/minimum interleukin (IL)-2 promoter, and subcloned into pRV-mCD19CAR to create pRV-mCD19CAR-Fla plasmids. Modified MIGR1 plasmids without IRES-GFP were used as control retroviral vectors (pRV-Mock). Afterward, the mCD19 scFv sequences in the pRV-mCD19CAR and pRV-mCD19CAR-Fla plasmids were replaced with a previously published human CD19-targeting (hCD19) scFv (derived from clone FMC63) sequences,<sup>17</sup> to construct hCD19 CAR plasmids.

To prepare CAR vectors for human CAR-T cell production, the CAR sequence with scFv targeting hCD19 (clone FMC63), CD8 transmembrane domain, 4-1BB costimulatory signal and CD3ζ domain, was constructed as described previously.<sup>18</sup> The sequence was cloned into a third-generation self-inactivating lentiviral vector under the control of the EF1α promoter to generate pLV-hCD19CAR plasmids. Similarly, the 4×NFAT promoter and codon-optimized Fla sequence were subcloned into pLV-hCD19CAR plasmid to generate pLV-hCD19CAR-Fla plasmids. Parental lentiviral plasmids were used as control vectors (pLV-Mock) to generate human mock T cells. All sequence synthesis and sequencing verification were accomplished by GENEWIZ (China).

### Murine T-cell isolation and CAR-T cell production

Mouse spleen T cells were isolated using a mouse CD3 T Cell Isolation Kit (BioLegend) from 6 to 8 weeks old C57BL/6J mice. T cells were then activated for 2 days using a plate coated with anti-mouse CD3 antibody (5 µg/mL, BioLegend, clone: 145–2C11), soluble anti-mouse CD28 (2 µg/mL, BioLegend, clone: 37.51) antibody and 50 U/mL murine IL-2 (PeproTech) in RPMI-1640 medium (Gibco) supplemented with 10% FBS, 2 mM GlutaMAX, 50 µM β-mercaptoethanol, 100 U/mL penicillin and 100 µg/mL streptomycin. T cells were infected with retroviral supernatants using RetroNectin-coated plates (Takara). On day 5, transduction efficiency was evaluated by staining the flag co-expressed with CAR using an allophycocyanin (APC)-conjugated anti-flag antibody (BioLegend). T cells were then harvested and used for further assays.

### Human T-cell isolation, culture and transduction

Peripheral blood mononuclear cells (PBMCs) were obtained from Milestone Biotech (Shanghai, China). Lentivirus supernatants used to transduce human T cells were prepared as previously described.<sup>19</sup> PBMCs were activated with anti-CD3/CD28 magnetic beads (T&L BioTech) and cultured in Roswell Park Memorial Institute (RPMI)-1640 medium supplemented with 10% FBS, 100 U/mL rhIL-2 (T&L BioTech), 1 mM sodium pyruvate. 48 hours later, pre-activated PBMCs were transduced using lentivirus supernatants with the assistance of polybrene (8 µg/mL). Flow cytometry was used to determine transduction effectiveness 3 days after infection, using the APC-conjugated anti-flag antibody (BioLegend). T cells were expanded in vitro for another 7 days before being used for experiments.

### Flagellin expression in CAR-T cells

Murine and human CAR(Flag)-T cells, as well as their respective control cells, were co-cultured with mCD19<sup>+</sup>B16F10 or hCD19<sup>+</sup>HCT116 cells at a ratio of 2:1 for 24 hours. Brefeldin A (Solarbio) was given to the co-cultures to block Flag secretion for an additional 8 hours. The cells were then stained with FITC-conjugated anti-His-tag antibody (BioLegend) and APC-conjugated anti-mouse CD3 antibody (BD) or human CD3ε antibody (BioLegend) to detect Flag expression in T cells. Flag levels in co-culture supernatants were also detected by western blot using an anti-6×His tag mouse monoclonal antibody (Proteintech).

### Cytotoxicity assay

The cytotoxicity assay was performed using luciferase-expressing target cells. In brief, the CAR-engineered T cells were co-cultured with matching target cells (eg, mCD19<sup>+</sup>B16F10 for murine CAR-T cells, hCD19<sup>+</sup>HCT116 for human CAR-T cells) at indicated ratios. Luciferase activity was employed as an indicator of target cell viability, and the luminous signal was detected by an Omega multifunctional microplate reader (BMG LABTECH), which used D-Luciferin potassium salt (Beyotime) as the substrate.

### Cytokine release

Mouse or human T cells were co-cultured with their corresponding target cells for 24 hours, then the supernatants were harvested to measure the secretion of interferon (IFN)-γ and IL-2. Likewise, to measure DC activation, mouse and human DCs were treated with 20 ng/mL Flag. After 24 hours, the supernatants were collected to detect IL-12 secretion. These cytokines were detected using ELISA kits (4A Biotech) following the manufacturer's instructions.

### Proliferation analysis

Engineered murine T cells were co-cultured with target cells at a ratio of 2:1. After 48 hours, T cells were collected and washed twice with phosphate-buffered saline (PBS) containing 1% bovine serum albumin (BSA), then stained with FITC-conjugated anti-mouse CD3 antibody

(BioLegend). Following that, cells were washed three times with PBS, fixed at -20°C for 1 hour using precooled 70% ethanol, and stained with APC-conjugated anti-mouse Ki-67 antibody (BioLegend) according to standard intracellular staining protocol. Similarly, human T-cell proliferation was detected using Brilliant Violet 510-conjugated anti-human Ki-67 antibody (BioLegend).

### Gene expression analysis for macrophages and DCs

Engineered murine and human T cells were co-cultured with their corresponding target cells (mCD19<sup>+</sup>B16F10 for murine T cells and hCD19<sup>+</sup>HCT116 for human T cells) at a ratio of 2:1 for 48 hours, and the supernatant was collected to stimulate prepared monocytes, macrophages and DCs. After 24 hours, the cells were harvested to detect active genes or phenotypic markers by quantitative real-time PCR. The primers used were provided in online supplemental table 1.

### Animal studies

6–8-week-old female C57BL/6J mice were used for all studies and maintained in individually ventilated cages under 12 hours of light/dark cycles in a specific pathogen-free animal facility. All animal procedures were approved by the Institutional Animal Care and Use Committee (IACUC) of Shenzhen Institutes of Advanced Technology, Chinese Academy of Sciences (Shenzhen, China. SIAT-IACUC-240227-YYX-WXC-A2483).

Female C57BL/6J mice were inoculated subcutaneously with 1×10<sup>6</sup> mCD19<sup>+</sup>B16F10, mCD19<sup>+</sup>MC38, hCD19<sup>+</sup>B16F10 or hCD19<sup>+</sup>MC38 cells in 100 µL Dulbecco's phosphate-buffered saline (DPBS) into the right flank to create a solid tumor model, or injected subcutaneously with a mixture (1:1 ratio) of mCD19<sup>+</sup>B16F10 and mCD19<sup>+</sup>B16F10 cells to create heterogeneous tumor models. Mice were randomly assigned 7 days later when the tumors had grown to approximately 100 mm<sup>3</sup>. Then, the mice were treated with 1×10<sup>7</sup> T cells injected into their lateral tail veins. To deplete macrophage in mice, 200 µL of clodronate liposomes (LIPOSOMA) was administered intravenously to each mouse 2 days before T-cell infusion.

To assess antitumor efficacy, the animals were individually monitored for tumor growth and body weight until humane endpoints were reached or the tumor volume exceeded the endpoint volume (1,500 mm<sup>3</sup>). Tumor size was calculated as volume=length×width<sup>2</sup>/2. Tumor samples were collected to detect the TME landscape using fluorescence-activated cell sorting (FACS) or immunohistochemistry. In addition, mice's spleens were collected on day 10 after T-cell infusion to investigate endogenous CD8<sup>+</sup>T cell responses.

### Analysis of endogenous CD8<sup>+</sup>T cell responses

Mouse spleen CD8<sup>+</sup>T cells were isolated using the MojoSort mouse CD8<sup>+</sup>T Cell Isolation Kit (BioLegend), and co-cultured with B16F10 cells at a ratio of 2:1 for 24 hours. Cytotoxicity and IFN-γ secretion were detected as previously described. Alternatively, CD8<sup>+</sup>T cells were



stimulated with nanoparticles loaded with B16F10 whole-cell antigen (Absin Biotech) for 32 hours before being exposed to brefeldin A for an additional 4 hours. IFN- $\gamma$ <sup>+</sup>CD8<sup>+</sup>T cells were detected by flow cytometry.

### Statistical analyses

Statistical analyses were analyzed using GraphPad Prism V.8.0 (GraphPad Software) and data were presented as mean $\pm$ SD. Statistical differences among groups were performed using the t-test and an analysis of variance comparison. Survival curves were analyzed using the log-rank test. A p value of <0.05 was considered statistically significant.

## RESULTS

### CAR-T cells expressing flagellin exhibited superior antitumor efficacy in vivo

To employ Fla's immune-stimulatory action while avoiding the potential safety hazards associated with systemic distribution, we generated murine CD19-targeted CAR-T cells that secrete Fla under the control of an inducible promoter on T-cell activation, which is referred to as CAR(Fla)-T cells (figure 1A). Mouse melanoma B16F10 cells that expressed murine CD19 (mCD19<sup>+</sup>B16F10) were employed as the target cells (figure 1B). As expected, CAR(Fla)-T cells produced Fla only on the recognition of target-positive cells and activation (figure 1C,D, online supplemental figure S1A). To assess if autocrine Fla enhances the function of CAR-T cells, we performed a cytotoxicity assay at various effector-to-target (E:T) ratios. However, Fla did not enhance the cytotoxicity of CAR-T cells against tumor cells in vitro (figure 1E) or boost the secretion of IL-2 and IFN- $\gamma$  (figure 1F). Furthermore, there was no significant difference in Ki67 expression between CAR(Fla)-T cells and conventional CAR-T cells, indicating that Fla had no impact on CAR-T cell proliferation (figure 1G). These findings suggest that Fla secretion by murine CAR-T cells does not influence their functions in vitro.

To investigate Fla's potential in boosting the anti-tumor activity of CAR-T cells in vivo, we established a syngeneic mCD19<sup>+</sup>B16F10 melanoma model in immune-competent mice. Following tumor cell implantation, engineered murine T cells were intravenously administered to tumor-bearing mice. Subsequently, the tumor volume and body weight were continuously monitored, and tumor tissues were collected for analysis on day 10 post-infusion (figure 1H). Surprisingly, in vivo findings demonstrated that CAR(Fla)-T cells effectively controlled tumor growth and considerably prolonged the survival of tumor-bearing mice compared with conventional CAR-T cells (figure 1I–K, online supplemental figure S1B). Mice treated with CAR(Fla)-T cells showed higher levels of IL-2, IFN- $\gamma$ , IL-1 $\beta$  and tumor necrosis factor (TNF)- $\alpha$  in tumor tissues than those treated with conventional CAR-T cells (figure 1L,M), substantiating that CAR(Fla)-T cells have more potent antitumor activity in vivo. Both CAR(Fla)-T

cells and conventional CAR-T cells displayed similar alterations in body weight (online supplemental figure S1C), indicating no significant difference in potential toxicity.

Next, we used a syngeneic colorectal carcinoma model based on mCD19<sup>+</sup>MC38 cells to demonstrate that our engineered T cells could be applied to treat more solid tumors. Similarly, the engineered murine CAR-T cells were given intravenously and tumor tissues were harvested on day 18 for analysis (figure 1N). Notably, CAR(Fla)-T cells effectively controlled MC38 tumor growth and prolonged the survival of tumor-bearing mice (figure 1O–Q, online supplemental figure S1D,E). Around 33% of mice treated with CAR(Fla)-T cells achieved tumor-free status, a result not observed with conventional CAR-T cell therapy. These findings underscore the feasibility of equipping CAR-T cells with Fla to improve their antitumor potential in solid tumors.

### CAR(Fla)-T cells outperform conventional CAR-T cells in vivo regardless of the target and are not affected by circulating flagellin-neutralizing antibodies

To further clarify the efficacy of our engineered CAR-T cells were not dependent on the nature of target antigens, we overexpressed human CD19 (hCD19) in B16F10 mouse melanoma cells (hCD19<sup>+</sup>B16F10) and MC38 colorectal carcinoma cells (hCD19<sup>+</sup>MC38) and employed them to establish syngeneic tumor mouse models. Following the infusion of CAR-T cells targeting hCD19, we observed that both CAR-T cell populations persisted in vivo for several days with no significant differences in their numbers (online supplemental figure S2A). However, CAR(Fla)-T cells consistently demonstrated superior antitumor activity compared with conventional CAR-T cells, as shown in both melanoma (figure 2A–C, online supplemental figure S2B) and colorectal carcinoma (figure 2D–F, online supplemental figure S2D). Additionally, we evaluated the therapeutic effect of intratumoral Fla administration combined with CAR-T therapy in both tumor models. The results showed that a single intratumoral injection of Fla, when combined with CAR-T therapy, had a weaker effect on tumor growth and mouse survival compared with CAR(Fla)-T cell therapy (online supplemental figure S2C,E). These data confirmed that CAR(Fla)-T cells perform better than CAR-T cells in vivo, even when combined with intratumoral Fla injection, regardless of the tumor antigen feature. We also thought about the possibility that Fla's potential immunogenicity could compromise this strategy's effectiveness. We examined the presence of CAR-T cells in the blood since potential immunogenicity could lead to their elimination by endogenous immune cells, and discovered that Fla expression did not impair the persistence of CAR(Fla)-T cells in vivo (online supplemental figure S2F). Moreover, to further confirm the feasibility of CAR(Fla)-T cells in patients with tumor who suffered infection with gram-negative bacteria (eg, *Salmonella*) previously and had high levels of circulating neutralizing antibodies against Fla, we immunized mice with recombinant Fla vaccines

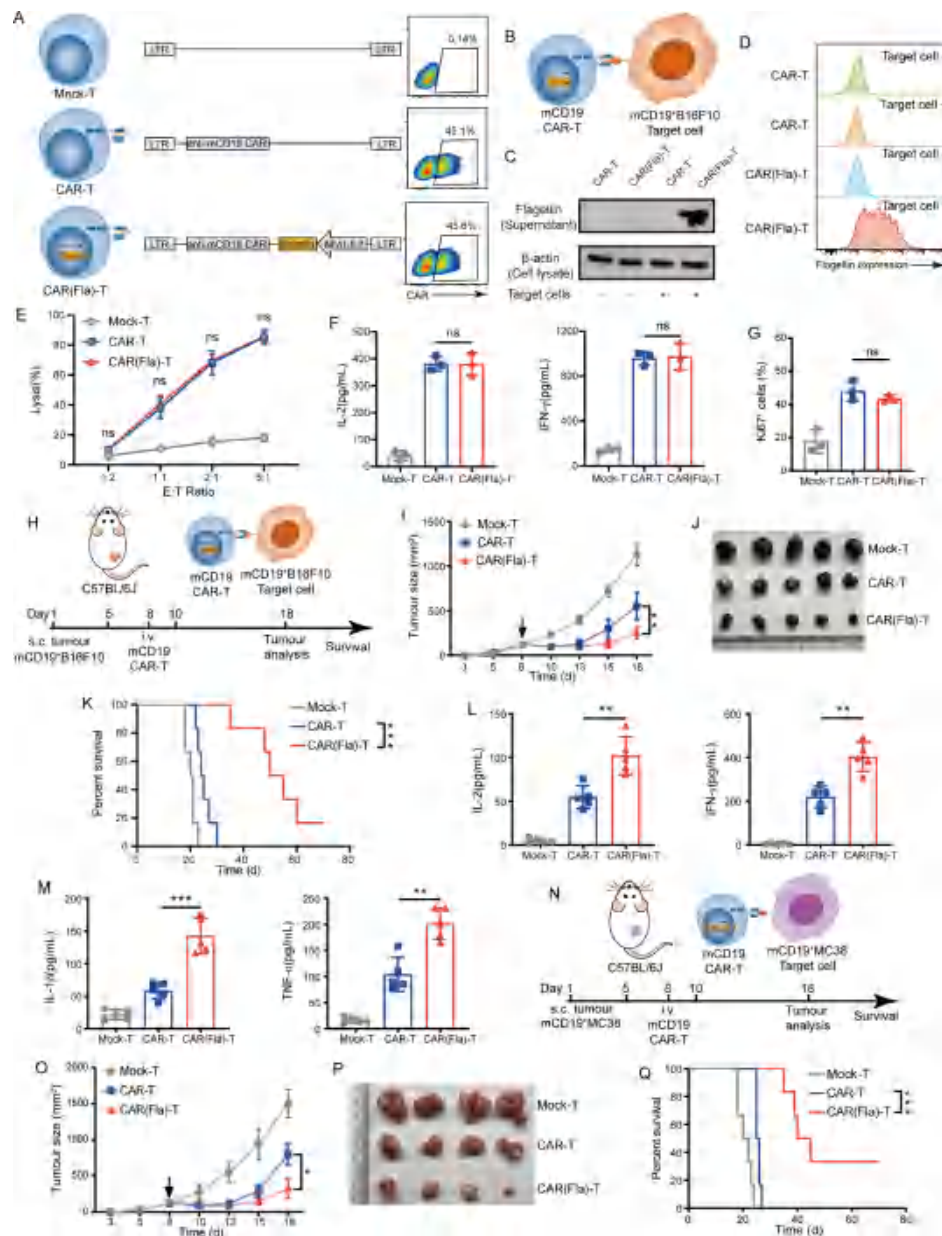


**Figure 1** CAR-T cells expressing flagellin exhibited superior antitumor efficacy in vivo. (A) Retroviral constructs used for murine T-cell engineering, and representative flow cytometry plots of CAR expression in engineered T cells. (B) Illustration of the interaction between CAR-T cells targeting murine CD19 and target cells (mCD19<sup>+</sup>B16F10). (C–D) Western blot (C) and flow cytometry (D) analysis of flagellin expression in CAR-T cells on target cell recognition. (E) Cytotoxicity analysis of engineered T cells against target tumor cells. Engineered T cells were co-cultured with mCD19<sup>+</sup>B16F10 cells at the indicated effector-to-target (E/T) ratios for 12 hours before analysis. ns, not significant. (F) ELISA assay for IL-2 and IFN- $\gamma$  secretion of engineered T cells when they were co-cultured with target cells at an E/T ratio of 2:1 for 24 hours. ns, not significant. (G) FACS analysis demonstrating the expression of Ki67 in engineered T cells. T cells were co-cultured with target cells at the E/T ratio of 2:1 for 48 hours before being analyzed. ns, not significant. (H) Engineered T-cell treatment schedule for subcutaneous murine B16F10 melanoma expressing murine CD19. (I) Measurement of tumor volume after tumor engraftment in mice (n=11 mice/group). The arrow indicates the time at which mice get intravenous infusions of engineered T cells. \*\*p<0.01. The arrow indicates the time point of intravenous injection of T cells. (J) Images of tumor tissue were recorded 10 days following engineered T-cell infusions, n=5 mice per group. (K) The Kaplan-Meier survival curves for tumor-bearing mice treated with engineered T cells. n=6 mice/group. \*\*\*p<0.001. (L–M) The quantities of IL-2, IFN- $\gamma$ , IL-1 $\beta$  and TNF- $\alpha$  in tumor lysates were evaluated by ELISA. \*\*\*p<0.001, \*\*p<0.01. (N) Engineered T-cell treatment schedule for subcutaneous murine colorectal carcinoma MC38 cells that express murine CD19. (O) Measurement of tumor volume after tumor engraftment in mice (n=8 mice/group). The arrow indicates the time at which mice get intravenous infusions of engineered T cells. \*p<0.05. The arrow indicates the time point of intravenous injection of T cells. (P) Images of tumor tissue taken 10 days after the infusion of engineered T cells. n=4 mice/group. (Q) The Kaplan-Meier survival curves for MC38 tumor-bearing mice treated with engineered T cells. n=4 mice/group. \*\*\*p<0.001. CAR, chimeric antigen receptor; FACS, fluorescence-activated cell sorting; Fla, flagellin; IFN, interferon; IL, interleukin; i.v., intravenous; s.c., subcutaneous; TNF, tumor necrosis factor.

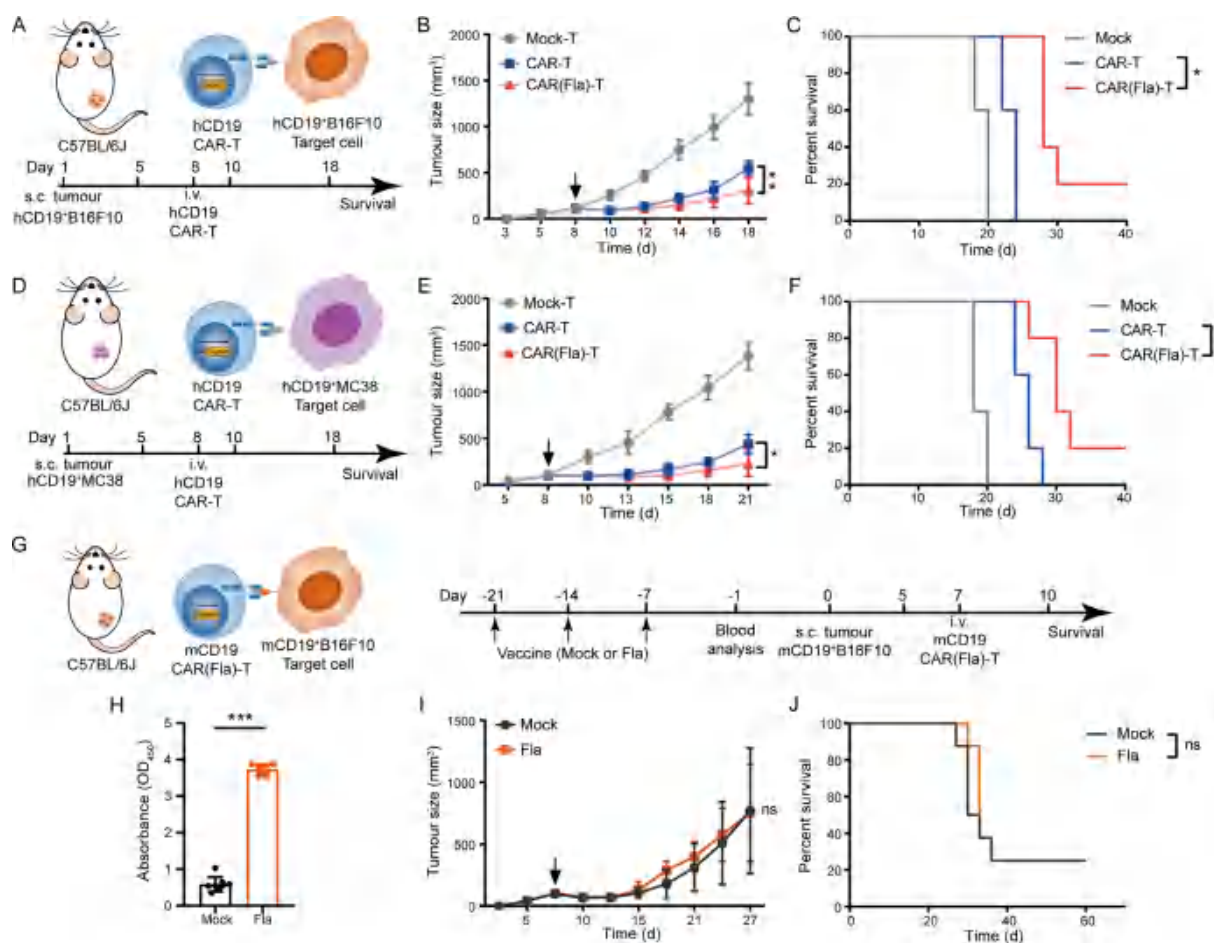


**Figure 2** Flagellin can improve the antitumor effects of CAR-T cells in different solid tumors. (A) Treatment schedule for subcutaneous murine B16F10 melanoma expressing human CD19 using engineered T cells. (B) The changes in tumor volume over time after tumor cell implantation,  $n=5$  mice/group,  $**p<0.01$ . The arrow indicates the time point of intravenous injection of T cells. (C) The Kaplan-Meier survival curves after treatment for B16F10 tumor-bearing mice.  $n=5$  mice/group,  $*p<0.05$ . (D) Treatment schedule for subcutaneous murine MC38 colorectal carcinoma expressing human CD19 by engineered T cells. (E) The changes in tumor volume over time after tumor cell implantation,  $n=5$  mice/group,  $*p<0.05$ . The arrow indicates the time point of intravenous injection of T cells. (F) The Kaplan-Meier survival curves after treatment for MC38 tumor-bearing mice,  $n=5$  mice/group,  $*p<0.05$ . (G) Experimental schedule with immunization prior to subcutaneous mCD19<sup>+</sup>B16F10 implantation and subsequent treatment with engineered T cells. (H) ELISA assay showing anti-flagellin antibody levels in the blood of mice post-vaccination,  $n=8$  mice/group,  $***p<0.001$ . (I) The changes in tumor volume over time after tumor cell implantation,  $n=8$  mice/group. ns, not significant. The arrow indicates the time point of intravenous injection of T cells. (J) The Kaplan-Meier survival curves following treatment for tumor-bearing mice,  $n=8$  mice/group, ns, not significant. CAR, chimeric antigen receptor; Fla, Flagellin; i.v., intravenous; s.c., subcutaneous.

before tumor cell implantation (figure 2G). As expected, there was a high titer of anti-Fla antibodies in the serum of immunized mice (figure 2H); however, this did not lessen the therapeutic efficacy of CAR(Fla)-T cells in vivo (figure 2I,J, online supplemental figure S2G). These findings suggest that CAR(Fla)-T cells can function effectively in vivo regardless of tumor target, Fla's potential immunogenicity or the presence of neutralizing antibodies.

#### Flagellin secreted by CAR-T cells can reshape the TME and encourage endogenous antitumor response

To confirm the superior antitumor effects of CAR(Fla)-T cells, tumor-infiltrating T cells were analyzed by immunohistochemistry, which revealed that more T cells were infiltrated in the tumors of CAR(Fla)-T cell-treated mice than those treated with conventional CAR-T cells

(figure 3A). Further investigation into the nature of infiltrated immune cells found that mice treated with CAR(Fla)-T cells had a larger percentage of CD8<sup>+</sup> T cells within the tumors (figure 3B, online supplemental figure S3A). These tumor-infiltrating CD8<sup>+</sup>T cells exhibited an antigen-experienced memory-like (CD62L<sup>+</sup>CD44<sup>+</sup>) phenotype and were more degranulated (CD107a<sup>+</sup>) than those isolated from conventional CAR-T cell-treated mice (figure 3C,D, online supplemental figure S3B,C). CAR-T cell exhaustion/dysfunction presents a significant challenge to CAR-T cell therapy.<sup>20</sup> Exhausted T cells have lower proliferative and cytokine-producing capacity, higher apoptosis rate and increased expression of inhibitory receptors, such as programmed cell death protein 1 (PD1), T cell immunoglobulin and mucin



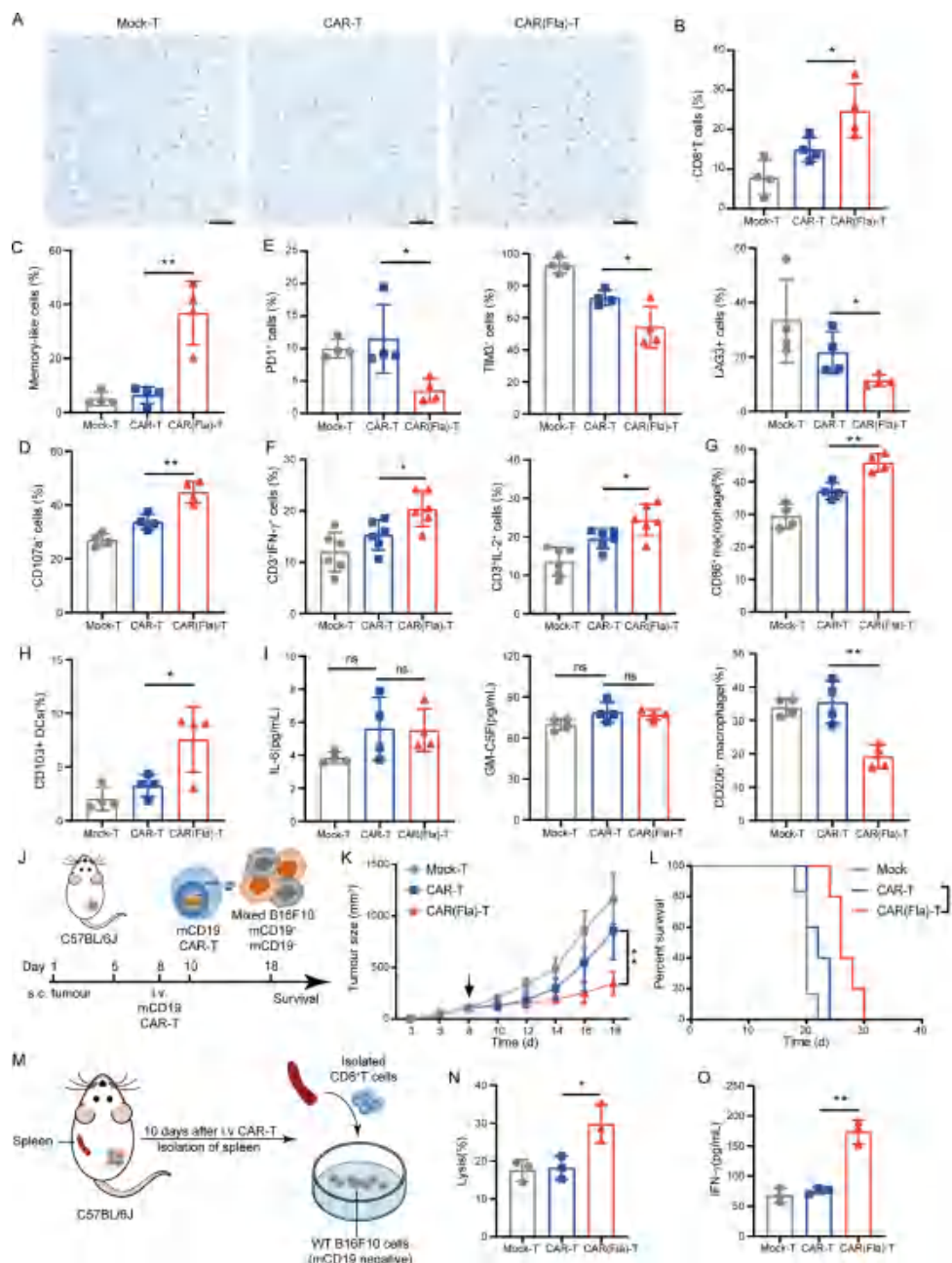


**Figure 3** Flagellin secreted by CAR-T cells can reshape the tumor microenvironment in vivo. (A) Representative images of immunohistochemistry staining for mouse CD3<sup>+</sup>T cells in tumor tissues. Scale bars, 50  $\mu$ m. (B–E) Characteristics of tumor-infiltrating CD8<sup>+</sup>T cells on day 18 post-implantation. The percentages of CD8<sup>+</sup>T cells (B), memory-like (CD44<sup>+</sup>CD62L<sup>+</sup>) CD8<sup>+</sup>T cells (C), CD107a<sup>+</sup>CD8<sup>+</sup>T cells (D) and exhaustion-like (PD1<sup>+</sup>, TIM3<sup>+</sup> or LAG3<sup>+</sup>) CD8<sup>+</sup>T cells (E) among treated groups are shown. All the samples were gated on CD45<sup>+</sup>CD3<sup>+</sup>CD8<sup>+</sup>T cells. \* $p$ <0.05, \*\* $p$ <0.01. (F) The percentages of tumor-infiltrating CD3<sup>+</sup>IFN- $\gamma$ <sup>+</sup> and CD3<sup>+</sup>IL-2<sup>+</sup>T cells on day 18, \* $p$ <0.05. All the samples were gated on CD45<sup>+</sup>CD3<sup>+</sup> cells. (G) The percentages of tumor-infiltrating CD206<sup>+</sup> (M2 type macrophages) or CD86<sup>+</sup> (M1 type macrophages), \*\* $p$ <0.01. All the samples were gated on CD45<sup>+</sup>CD11b<sup>+</sup>F4/80<sup>+</sup> cells. (H) The percentages of tumor-infiltrating CD103<sup>+</sup>DCs cells on day 18, \* $p$ <0.05. All the samples were gated on CD45<sup>+</sup>CD11c<sup>+</sup> cells. (I) IL-6 and GM-CSF levels in murine blood were analyzed using ELISA. (J) Treatment schedule for the mixed tumor model with 50% of murine B16F10 melanoma cells expressing murine CD19. (K) The changes in tumor volume over time after tumor cell implantation,  $n=5$  mice/group, \*\* $p$ <0.01. The arrow indicates the time point of intravenous injection of T cells. (L) The Kaplan-Meier survival curves following treatment for tumor-bearing mice,  $n=5$  mice/group, \*\* $p$ <0.01. (M) Illustration depicting the analysis of endogenous CD8<sup>+</sup>T cell activity. WT, wild type. (N) Cytotoxicity analysis of splenic CD8<sup>+</sup>T cells against WT B16F10 cells. T cells were co-cultured with B16F10 cells at an E/T ratio of 2:1 for 24 hours prior to analysis, \* $p$ <0.05. (O) IFN- $\gamma$  secretion in the supernatant of CD8<sup>+</sup>T cells co-cultured with target cells for 24 hours at an E/T ratio of 2 to 1 was measured by ELISA, \*\* $p$ <0.01. CAR, chimeric antigen receptor; E:T, effector-to-target; Fla, flagellin; GM-CSF, granulocyte macrophage-colony stimulating factor; IFN, interferon; IL, interleukin; i.v., intravenous; LAG3, lymphocyte activation gene 3; PD1, programmed cell death protein 1; s.c., subcutaneous; TIM3, T cell immunoglobulin and mucin domain-containing protein 3.

domain-containing protein 3 (TIM3) and lymphocyte activation gene 3 (LAG3). Therefore, we also analyzed the exhausted/dysfunctional phenotype of tumor-infiltrating CD8<sup>+</sup>T cells and discovered that CAR(Flag)-T cell-treated mice had a much lower proportion of CD8<sup>+</sup>T cells expressing inhibitory receptors (PD1, TIM3 and LAG3) (figure 3E, online supplemental figure S3D), but contained higher levels of IFN- $\gamma$ <sup>+</sup> and IL-2<sup>+</sup>T cells (figure 3F, online supplemental figure S3E). Similarly, CAR(Flag)-T cell-treated mice exhibited higher levels of IL-2 and IFN- $\gamma$  in the tumors (online supplemental figure S3F).

To further investigate this effect, we generated CAR-T cells co-expressing green fluorescent protein (GFP) to assess their intratumoral distribution and functional status (online supplemental figure S4A). GFP-positive CAR-T cells were detected within tumors 48 hours post-infusion. Notably, tumors treated with CAR(Flag)-T cells exhibited a significantly higher proportion of GFP-positive CAR-T cells compared with those treated with control CAR-T cells (online supplemental figure S4B), alongside elevated levels of Fla (online supplemental figure S4C). Further phenotypic analysis of intratumoral CAR-T cells demonstrated that CAR(Flag)-T cells displayed a greater proportion of central memory-like phenotypes (online supplemental figure S4D) and a lower exhaustion state (online supplemental figure S4D) compared with conventional CAR-T cells. Moreover, while the proportion of CD107a<sup>+</sup> CAR(Flag)-T cells showed a tendency to be higher than that of CD107a<sup>+</sup> CAR-T cells, this difference was not statistically significant (online supplemental figure S4F). This may be attributable to the strong cytotoxic activity of both CAR-T cell types during the early stages of the antitumor immune response, during which the indirect effects of Fla had not yet exerted a substantial impact.

Considering that autocrine Fla could not affect the function of CAR-T cells in vitro, we hypothesized that Fla might enhance the antitumor effects of CAR-T cells in vivo by affecting other immune cells in the TME. Therefore, non-T lymphocytes, particularly TLR5-expressing innate immune cells in the TME were also analyzed.<sup>21</sup> Flow cytometry analysis demonstrated a prevalence of CD206<sup>+</sup>M2-like macrophages in tumor tissues initially. Following CAR(Flag)-T cell treatment, the population of M2-type macrophages decreased whereas the CD86<sup>+</sup>M1-type macrophages increased (figure 3G, online supplemental figure S4G). Similarly, CAR(Flag)-T cell-treated mice had greater levels of IL-1 $\beta$ , TNF- $\alpha$  and nitric oxide (NO) content in tumor tissues than those treated with conventional CAR-T cells (online supplemental figure S4H,I). These data suggested CAR-T cell-derived Fla can drive macrophage to shift from M2 to M1 phenotype. Moreover, we also discovered that mice treated with CAR(-Fla)-T cells exhibited increased infiltration of CD103<sup>+</sup>DCs and elevated levels of IL-12 in tumors, indicating Fla also heightened DCs activation within the tumors (figure 3H, online supplemental figure S4J,K). Mice treated with

either conventional CAR-T cells or CAR(Flag)-T cells had quite low levels of IL-6 and GM-CSF in the peripheral blood, indicating these two CAR-T therapies have an extremely low risk of cytokine storms (figure 3I). Collectively, these findings suggest that Fla expression by engineered CAR-T cells can reshape the TME to establish an “immune-hot” milieu by promoting macrophage polarization and DCs activation.

Antigenic heterogeneity is another significant barrier to the success of CAR-T cell therapy in solid tumors.<sup>22</sup> CD103<sup>+</sup>DCs are critical for generating antitumor immune responses because they can cross-present tumor antigens produced from necrotic and apoptotic tumor cells.<sup>23</sup> Our results demonstrated that CAR(Flag)-T cell treatment increased the proportion and activation of CD103<sup>+</sup>DCs within tumors (figure 3H, online supplemental figure S4J,K), implying that it can promote endogenous antitumor immunity to overcome antigenic heterogeneity. To accomplish this, we employed a previously described antigenic heterogeneity model,<sup>24</sup> in which mice were subcutaneously injected with a 1:1 mixture of wild-type (antigen-negative) mCD19<sup>+</sup>B16F10 cells and (antigen-positive) mCD19<sup>+</sup>B16F10 cells (figure 3J). Compared with mice treated with conventional CAR-T cells, or CAR-T cells combined with intratumoral Fla administration, those treated with CAR(Flag)-T cells showed a significant reduction in tumor growth and prolonged survival (figure 3K and L, online supplemental figure S5A,B). Moreover, when co-cultured with mCD19<sup>+</sup>B16F10 cells or stimulated with nanoparticles loaded with B16F10 whole cell antigen—both of which do not express the CAR target antigen—the splenic CD8<sup>+</sup>T cells from CAR(Flag)-T cell-treated mice displayed significantly greater tumor-killing capacity and IFN- $\gamma$  secretion than those from conventional CAR-T-treated mice (figure 3M–O, online supplemental figure S5C,D). These findings support the notion that CAR(Flag)-T treatment can more effectively trigger endogenous CD8<sup>+</sup>T cell responses to combat tumors with antigenic heterogeneity.

### Flagellin secreted by CAR-T cells can favor M1 macrophage polarization and activate DCs

To further confirm the action of CAR-T cell-derived Fla on macrophage polarization, we stimulated mouse bone marrow-derived monocytes with the supernatant of CAR-T cells co-cultured with tumor cells in vitro (figure 4A). As expected, the results demonstrated that Fla effectively induced monocyte differentiation, upregulating the messenger RNA (mRNA) expression of markers specific to M1 macrophages (*Nos2* and *Cd86*) and downregulating those specific to M2 macrophages (*Arg1* and *Cd206*) (figure 4B). In addition, it elevated the mRNA levels of pro-inflammation cytokines (*Il-1 $\beta$*  and *Tnf- $\alpha$* ) while decreasing the levels of anti-inflammatory factors (*Il10* and *Tgfb $\beta$ 1*) (figure 4C). These data suggest that Fla can promote monocytes differentiated to M1 rather than M2-type macrophages. However, the majority of macrophages in the TME demonstrate an immunosuppressive M2 state



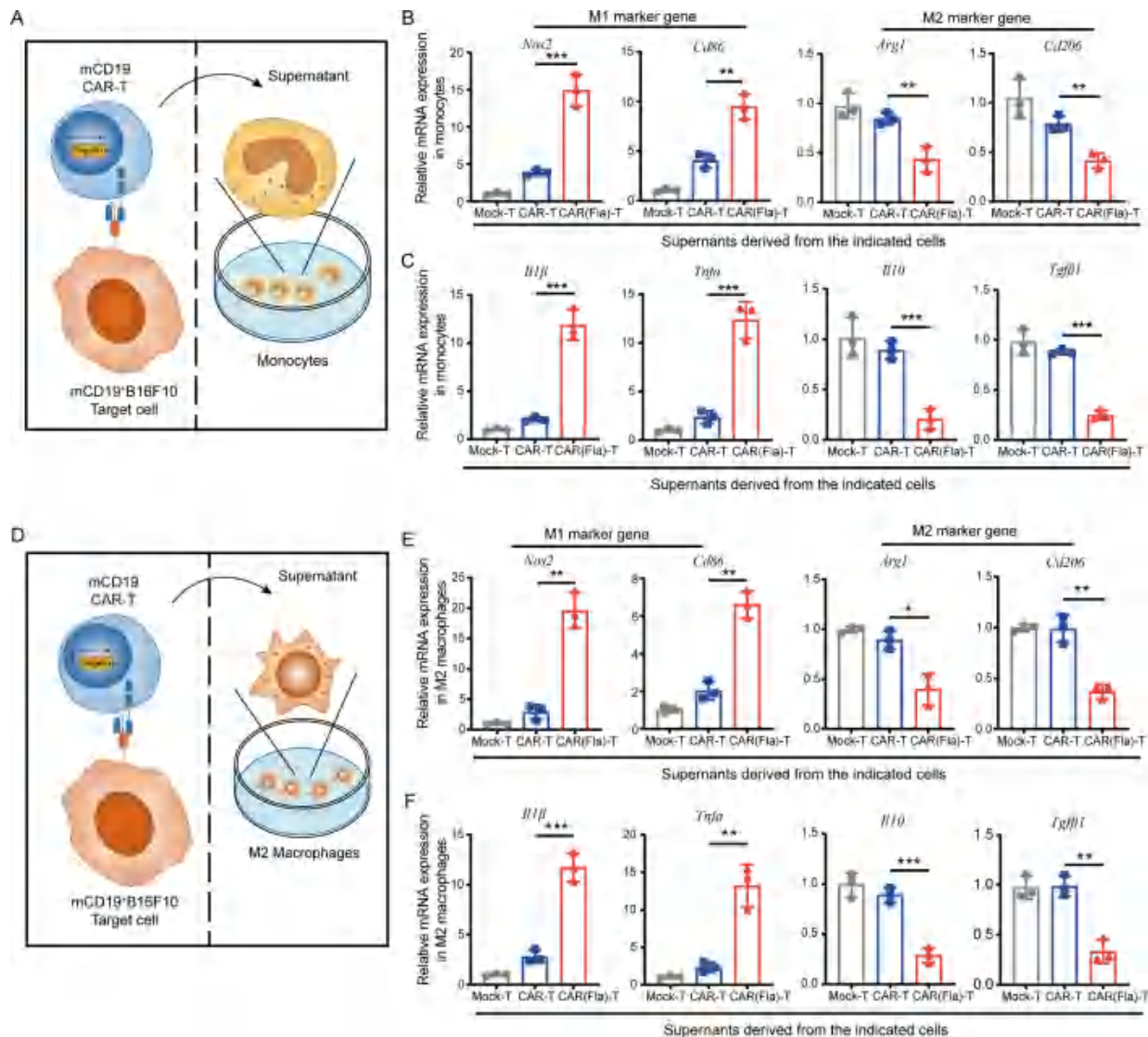


**Figure 4** Flagellin secreted by murine CAR-T cells can activate macrophages. (A) Illustration of experimental design for assessing monocyte activation in vitro. (B) M1 (*Nos2* and *Cd86*) and M2 (*Arg1* and *Cd206*) marker genes of macrophages were analyzed by qPCR, \*\*\*p<0.001, \*\*p<0.01. (C) Macrophage-associated pro-inflammatory (*Il-1β* and *Tnf-α*) and anti-inflammatory (*Il-10* and *Tgf-β1*) gene mRNA levels were analyzed by qPCR, \*\*\*p<0.001. (D) Illustration of experimental design for assessing M2-like macrophage activation in vitro. (E) M1 (*Nos2* and *Cd86*) and M2 (*Arg1* and *Cd206*) marker genes of macrophages were analyzed by qPCR, \*\*p<0.01, \*p<0.05. (F) Macrophage-associated pro-inflammatory (*Il-1β* and *Tnf-α*) and anti-inflammatory (*Il-10* and *Tgf-β1*) gene mRNA levels were analyzed by qPCR, \*\*\*p<0.001, \*\*p<0.01. CAR, chimeric antigen receptor; Fla, flagellin; mRNA, messenger RNA; qPCR, quantitative PCR.

(usually called TAM).<sup>25 26</sup> Whether Fla can reverse TAM polarization is crucial for the efficacy of immunotherapy. To this end, murine M2 macrophages were induced in vitro and then exposed to supernatant from CAR-T cells co-cultured with tumor cells (figure 4D). The quantitative PCR (qPCR) analysis revealed that CAR-T cell-derived Fla significantly upregulated the M1 while downregulated M2 macrophage-specific markers (figure 4E), which was accompanied by increased mRNA levels of antitumor cytokines and decreased levels of anti-inflammatory factors in macrophages (figure 4F). Additionally, we also assessed the impact of Fla secreted by CAR-T cells on DC activation in vitro and found that Fla stimulated DCs to produce more IL-12 (online supplemental figure S6A,B).

These results indicate that Fla secreted by CAR-T cells can effectively activate macrophages and DCs, encouraging the release of pro-inflammatory cytokines from them.

### Flagellin-activated macrophages and DCs enhance the antitumor effects of CAR-T cells

To investigate the possibility that Fla improves CAR-T cell function by activating macrophages and DCs, we generated recombinant Fla by employing the *Escherichia coli* recombinant protein expression system (online supplemental figure S6C), and used it to stimulate murine macrophages. Subsequently, the supernatant from Fla-activated macrophages was introduced into a co-culture system consisting of murine CAR-T cells and

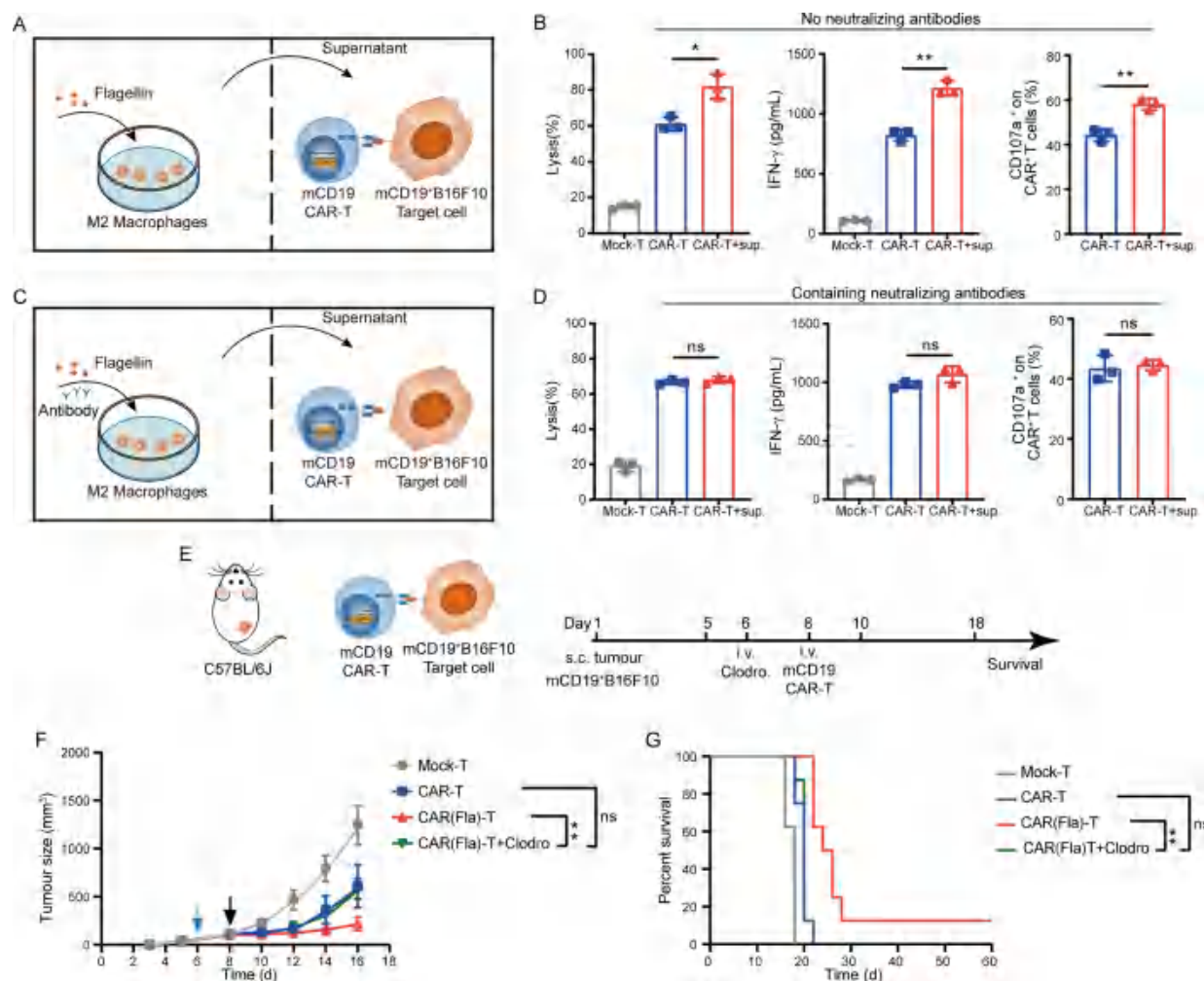


**Figure 5** Flagellin-activated macrophages enhance the antitumor effects of CAR-T cells. (A) Experimental design illustrating the co-culture of engineered T cells with mCD19<sup>+</sup>B16F10 in the presence of M2 macrophages supernatant for 24 hours at an E/T of 2 to 1. The supernatants were obtained from macrophages treated with flagellin. (B) Cytotoxicity, IFN- $\gamma$  secretion and the percentage of CD107a<sup>+</sup>CAR-T cells were detected after co-culture, \*\* $p < 0.01$ , \* $p < 0.05$ . (C) Experimental design illustrating the co-culture of engineered T cells with mCD19<sup>+</sup>B16F10 in the presence of macrophage supernatant for 24 hours at an E/T of 2 to 1. The supernatants were derived from macrophages treated with flagellin in the presence of flagellin-neutralizing antibodies. (D) Cytotoxicity, IFN- $\gamma$  secretion and the percentage of CD107a<sup>+</sup>CAR-T cells were detected after co-culture. ns, not significant. (E) Treatment schedule with macrophage depletion prior to treatment with engineered T cells in the mCD19<sup>+</sup>B16F10 tumor model. To deplete macrophage in mice, 200  $\mu$ L of clodronate liposomes (Clodro) was intravenously injected to each mouse 2 days prior to T-cell infusion. (F) The changes in tumor volume over time after mCD19<sup>+</sup>B16F10 cell implantation,  $n = 8$  mice/group, \*\* $p < 0.01$ , ns, not significant. The blue arrow indicates the time point of intravenous injection with clodronate liposomes. The black arrow indicates the time point of intravenous T-cell injection. (G) The Kaplan-Meier survival curves following treatment for tumor-bearing mice,  $n = 8$  mice/group, \*\* $p < 0.01$ , ns, not significant. CAR, chimeric antigen receptor; E:T, effector-to-target; Fla, flagellin; IFN, interferon; i.v., intravenous; s.c., subcutaneous.

mCD19<sup>+</sup>B16F10 tumor cells (figure 5A). The results indicated a significant enhancement by Fla-activated macrophage supernatant in the cytotoxicity of CAR-T cells against mCD19<sup>+</sup>B16F10 cells, accompanied by increased IFN- $\gamma$  secretion and a higher proportion of CD107a<sup>+</sup> CAR-T cells (figure 5B). When neutralizing antibody-containing serum was administered to Fla-stimulated macrophages, the supernatant failed to enhance the cytotoxic capabilities of CAR-T cells (figure 5C,D), validating the pivotal roles played by macrophages in Fla-mediated improvement of CAR-T function. Following a similar methodology, we investigated whether Fla-activated DCs

could boost the antitumor response of CAR-T cells, and the results revealed a significant increase in CAR-T cell function by the supernatant from activated DCs (online supplemental figure S6D,E). However, the use of Fla-neutralizing antibodies counteracted this heightened effect of activated DCs supernatant (online supplemental figure S6F). These results suggest that Fla-activated macrophages and DCs indirectly improve the antitumor effects of CAR-T cells.

Given the quantitative advantage of macrophages in the TME and the significant effects of Fla on their polarization, we tested whether Fla affected the antitumor

effects of CAR-T cells mainly through macrophages by employing clodronate liposomes to deplete macrophages in mice. Following macrophage depletion, the advantages of CAR(Fla)-T cells on tumor control and prolonged survival of tumor-bearing mice were markedly reduced (figure 5E–G, online supplemental figure S7A,B), underscoring the substantial reliance of CAR(Fla)-T cell function on the presence of macrophages. These findings imply that Fla promotes CAR-T cell function in vivo mostly through macrophages, while it can activate both macrophages and DCs simultaneously.

### Function of human CAR(Fla)-T cells is superior to conventional CAR-T cells in vitro

To evaluate the application potential of such a strategy in humans, we generated human CD19 CAR-T cells with inducible expression motifs that are capable of triggering Fla expression when the CAR is activated (figure 6A). HCT116 human colorectal carcinoma cells that overexpressed hCD19 antigen (hCD19<sup>+</sup>HCT116) were used as the target tumor cells (online supplemental figure S8A). As expected, CAR(Fla)-T cells expressed Fla only when they were co-cultured with target cells (figure 6B, online supplemental figure S8B,C). In vitro cytotoxicity assays showed that CAR(Fla)-T cells had much better tumor-killing capabilities than conventional CAR-T cells at high E:T ratios (figure 6C). In line with this, CAR(Fla)-T cells exhibited elevated levels of IL-2 and IFN- $\gamma$  (figure 6D), as well as upregulation of Ki67, a common marker of proliferation, when they were co-cultured with target cells (figure 6E). These data suggest that Fla could promote activation, proliferation and cytotoxicity of human CAR-T cells in vitro. It is worth noting that the effects of Fla on murine and human CAR-T cell function were inconsistent in vitro, which is potentially attributed to the presence of TLR5 on human CD4<sup>+</sup>T cells.<sup>27</sup> To address this issue, we generated CAR-T cells using CD8<sup>+</sup> T cells, as they lack TLR5 expression (online supplemental figure S8D). Cytotoxicity and cytokine secretion assays revealed that the potentiating effect of Fla on the antitumor activity of human CAR-T cells was lost in the absence of TLR5 (online supplemental figure S8E,F). Consistent results were observed when TLR5 was knocked out in CD4<sup>+</sup> CAR(Fla)-T cells or when a TLR5 antagonist was employed. Both approaches significantly abrogated the enhanced effects of autocrine Fla on cytokine production, including IL-2 and IFN- $\gamma$  (online supplemental figure S8G,H). This finding was further corroborated in NK cells, as Fla could not effectively improve the tumor-killing ability of mouse NK cells (online supplemental figure S8I), which lack TLR5 expression.<sup>28</sup> However, it was effective in enhancing the cytotoxicity of human NK cells (online supplemental figure S8I). This species-specific difference in TLR5 expression between mice and humans suggests that the novel CAR(Fla)-T therapy may hold greater clinical potential than initially anticipated.

Similarly, human CAR(Fla)-T cells and control CAR-T cells were separately co-cultured with hCD19<sup>+</sup>HCT116

cells. The supernatants from these cultures were then used to stimulate monocyte differentiation (online supplemental figure S8J). Analysis using qPCR revealed that supernatant from CAR(Fla)-T cells led to increased mRNA levels of M1 macrophage-specific markers (*NOS2* and *HLA-DRA*) and decreased levels of M2 macrophage-specific markers (*CD163* and *MRC1*) compared with supernatant from control CAR-T cells (online supplemental figure S8K). Additionally, mRNA levels of pro-inflammatory factors (*IL-1 $\beta$*  and *TNF $\alpha$* ) were higher, whereas levels of immunosuppressive factors (*IL-10* and *TGF $\beta$ 1*) were lower in cells treated with supernatant from CAR(Fla)-T cells compared with those treated with control supernatant (online supplemental figure S8L). These findings suggest that Fla secreted by human CAR-T cells prompts monocyte polarization toward an M1-like phenotype. To further explore the impact of Fla on human M2-like macrophages, we first induced macrophages to adopt an M2-like phenotype and then exposed them to the co-culture supernatant (figure 6F). Remarkably, supernatants containing Fla significantly increased M1 markers and decreased M2 markers in the macrophages, along with an upregulation of pro-inflammatory cytokines and a downregulation of anti-inflammatory cytokines (figure 6G,H). These results suggest that Fla released by human CAR-T cells can reprogram macrophages toward the M1 phenotype.

To evaluate how Fla-activated macrophages affect the antitumor activity of human CAR-T cells, we co-cultured human CAR-T cells with hCD19<sup>+</sup>HCT116 cells in the presence of supernatants from Fla-stimulated or control macrophages (online supplemental figure S9A). Our results showed that adding supernatant from Fla-stimulated macrophages enhanced the ability of CAR-T cells to lyse tumor cells and increased their secretion of IFN- $\gamma$  (figure 6I). These effects were reversed when neutralizing antibodies were added to deplete Fla from the medium (figure 6J). We then conducted similar experiments with human DCs, demonstrating that Fla released by human CAR-T cells could trigger DCs to secrete IL-12 (online supplemental figure S9B,C). Moreover, treating CAR-T cells with supernatants from Fla-activated DCs substantially boosted their capacity to kill tumor cells and produce IFN- $\gamma$  (online supplemental figure S9D,E), an effect that was diminished by administering neutralizing antibodies against Fla (online supplemental figure S9F). Taken together, these results indicate that human CAR(-Fla)-T cells exhibit enhanced cytotoxic and immunostimulatory abilities compared with conventional CAR-T cells, consistent with our observations in murine CAR-T cells.

### Discussion

One approach to augmenting antitumor immunity in the suppressive TME involves equipping T cells with synthetic receptors or pro-inflammatory cytokines that can reshape the TME favorably for antitumor response.<sup>4–6 29 30</sup> Targeting infiltrating immunosuppressive cells in tumors, such as TAMs, is receiving growing attention.<sup>31–35</sup> Here, we



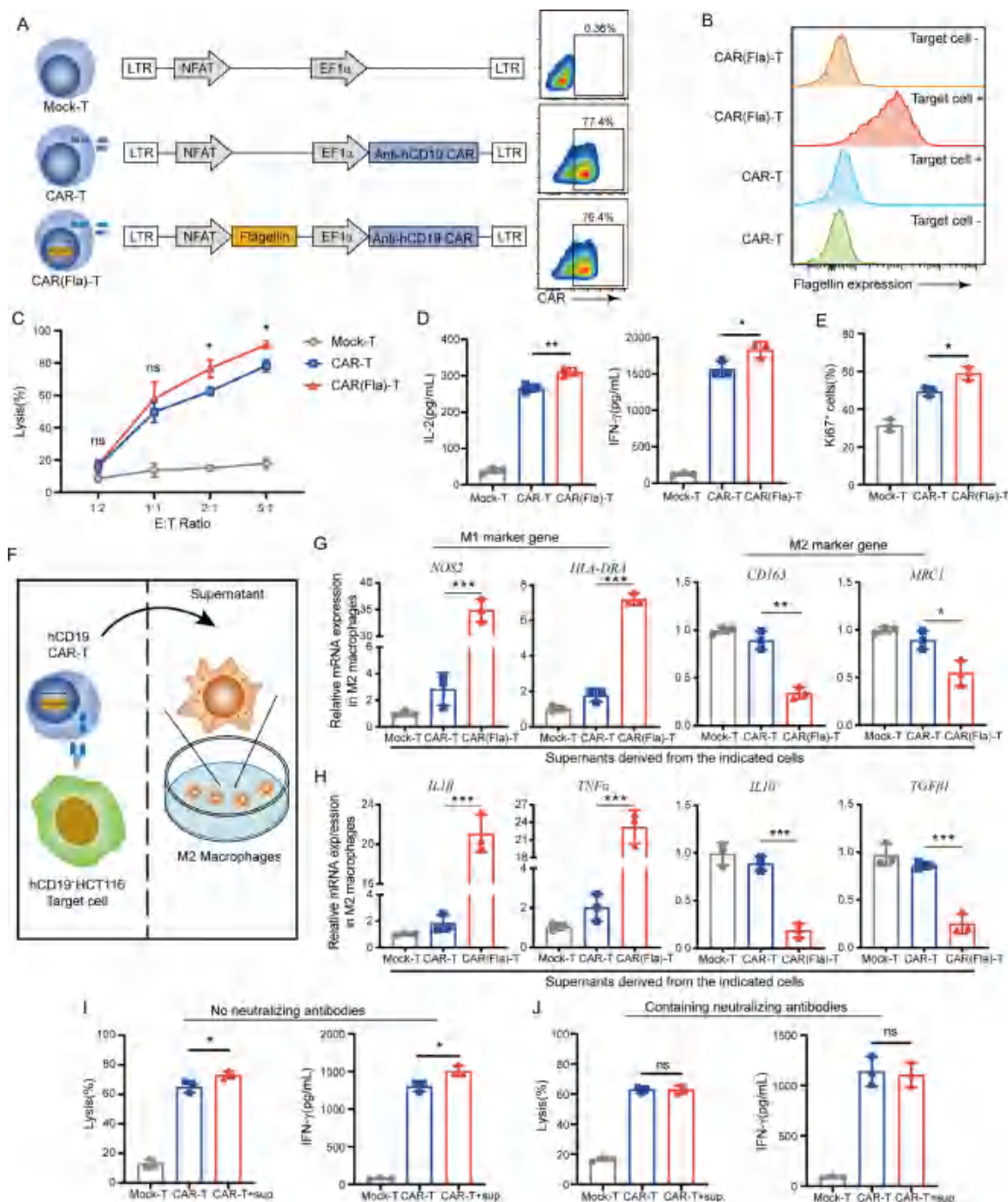


**Figure 6** Function of human CAR(Fla)-T cells is superior to conventional CAR-T cells in vitro. (A) Self-inactivating (ΔU3) lentiviral constructs used for human T-cell engineering, and representative flow cytometry plots of CAR expression in engineered human T cells. (B) Flow cytometry analysis of flagellin expression in CAR-T cells on target cell recognition. (C) Cytotoxicity assay of engineered T cells against hCD19<sup>+</sup>HCT116 cells, \*p<0.05, ns, not significant. Engineered T cells were co-cultured with target cells at the indicated E/T ratios for 12 hours prior to analysis. (D) ELISA assay for IL-2 and IFN-γ secretion of engineered T cells when they were co-cultured with target cells at an E/T ratio of 2:1 for 24 hours, \*\*p<0.01, \*p<0.05. (E) FACS analysis demonstrating the expression of Ki67 in engineered T cells, \*p<0.05. T cells were co-cultured with target cells at the E/T ratio of 2:1 for 48 hours before being analyzed. (F) Illustration of an experimental design for assessing the activation of M2-like macrophages in vitro. (G) M1 (*NOS2* and *HLA-DRA*) and M2 (*CD163* and *MRC1*) marker genes of macrophages were analyzed by qPCR, \*\*\*p<0.001, \*\*p<0.01, \*p<0.05. (H) Macrophage-associated proinflammatory (*IL-1β* and *TNF-α*) and anti-inflammatory (*IL-10* and *TGF-β1*) gene mRNA levels were analyzed by qPCR, \*\*\*p<0.001. (I–J) The engineered T cells were co-cultured with hCD19<sup>+</sup>HCT116 in the presence of macrophage supernatant for 24 hours at an E/T ratio of 2 to 1, followed by detection of cytotoxicity and IFN-γ secretion. The supernatants were obtained from macrophages treated with flagellin either without (I) or with (J) flagellin-neutralizing antibodies. \*p<0.05, ns, not significant. CAR, chimeric antigen receptor; E:T, effector-to-target; FACS, fluorescence-activated cell sorting; Fla, flagellin; IFN, interferon; IL, interleukin; mRNA, messenger RNA; qPCR, quantitative PCR; TGF, transforming growth factor; TNF, tumor necrosis factor.

engineered CAR-T cells to express Fla under the control of CAR signaling (referred to as CAR(Fla)-T cells) and assessed their antitumor effects. Our findings indicated that CAR(Fla)-T cells could impede tumor growth and extend the survival of tumor-bearing mice more effectively, since Fla can increase the ratio of M1-like macrophages and CD103<sup>+</sup>DCs within tumors, which established an immune-hot milieu. This feature enabled CAR(-Fla)-T cells to effectively activate endogenous CD8<sup>+</sup>T cell responses, which are crucial for controlling tumors with diverse antigens. While Fla activates both DCs and macrophages, the enhanced antitumor effects of CAR-T cells with Fla predominantly rely on macrophages. Depletion of macrophages significantly diminished the benefits of CAR(Fla)-T cells in tumor control and prolonged survival in tumor-bearing mice. This finding underscores the potential of targeting the TME to enhance CAR-T cell function effectively.

Fla is a protein that forms the structural component of flagella, the whip-like appendages that are responsible for *Salmonella* motility.<sup>36</sup> In the context of immunology, Fla is also known for its role as a potent activator of the immune system, particularly through its interaction with the TLR5 on immune cells.<sup>37</sup> Recently, it was demonstrated that activating the innate immune response with Fla can induce various effects on tumor growth in several experimental animal models.<sup>12 38</sup> Furthermore, previous studies have demonstrated that intratumoral injection or sustained delivery of Fla via T-cell loading can significantly enhance the antitumor efficacy of T-cell-based immunotherapies, with no toxicity observed during trials.<sup>14</sup> However, intratumoral injection poses accessibility challenges and is not feasible for all tumors, making clinical translation difficult. While continuous delivery through immune cells addresses the accessibility issue, the absence of built-in regulatory or termination mechanisms raises concerns about potential cumulative toxicity due to prolonged Fla exposure. To address this, we engineered Fla expression to be regulated by CAR signaling through the NFAT system. In the presence of tumor cells, CAR activation not only triggers T-cell cytotoxicity but also drives Fla expression, which remodels the TME to enhance CAR-T cell efficacy. Once the tumor is eliminated and CAR signaling ceases, Fla expression is also halted, minimizing the risk of prolonged Fla exposure. Furthermore, our findings show that CAR(Fla)-T cells outperform not only conventional CAR-T cells but also the combination of CAR-T cells with intratumoral Fla injection. This suggests that the TME is resistant to change and requires continuous Fla stimulation for effective remodeling, as single high-dose intratumoral Fla administration fails to achieve this. Additionally, the superiority of CAR(Fla)-T cells also lies in their dual role in supporting Fla-mediated TME remodeling. They not only serve as a source of Fla but also adapt to the TME reshaped by flagellin, enhancing their survival and thereby promoting further Fla production. This establishes a positive feedback loop that continuously drives TME remodeling. CAR(Fla)-T therapy therefore may be a more

straightforward and viable approach, offering a better balance of efficacy and safety compared with CAR-T cells alone or in combination with intratumoral Fla injection.

TAMs are the most prevalent immune cells found in solid tumors, and they typically display an M2-like phenotype that supports tumor cell survival, proliferation, and dissemination.<sup>39</sup> Activation of TLRs stimulates M1-polarized macrophage responses by initiating a proinflammatory program. Generally, converting TAMs to the M1 phenotype can provide therapeutic benefits by promoting antitumor immunity.<sup>26 39 40</sup> Engineered bacteria that secrete Fla can significantly activate M1 macrophages and reduce the proportion of M2-like macrophages in tumors, with TLR5-mediated signaling being crucial in this process.<sup>41</sup> Our findings indicate that Fla secreted by engineered CAR-T cells effectively activates macrophages and can convert M2 macrophages to the M1 phenotype, thereby remodeling the TME to enhance CAR-T cell function in vivo. Tumor cell death caused by CAR-T cells can spread tumor antigens, which might stimulate endogenous immune cell response against multiple tumor antigens.<sup>22</sup> Improving this process would be an appealing strategy for overcoming tumor heterogeneity and immune escape caused by antigen loss. CAR-T cells equipped with *Helicobacter pylori*-derived neutrophil-activating protein were proven to be capable of causing antigen spreading and thereby stimulating endogenous CD8<sup>+</sup> T-cell responses.<sup>24</sup> Our experimental results provide additional support for this viewpoint. Fla activates and recruits CD103<sup>+</sup>DCs, which are vital for generating endogenous antitumor immune responses because they can cross-present tumor antigens from necrotic and apoptotic tumor cells.<sup>23</sup> As a result, CAR (Fla)-T cells not only have their own superior antitumor effects but also activate endogenous T cells, making them more effective against tumors with diverse antigens. However, the enhanced antitumor function of CAR (Fla)-T cells in vivo was significantly reduced after macrophage depletion, indicating that Fla initially boosts the antitumor function of CAR-T cells through macrophages and subsequently activates CD103<sup>+</sup> DCs to induce an endogenous antitumor immune response. Our findings suggest that targeting intratumor macrophages could be more effective in reshaping the immunosuppressive TME.

Unlike murine T cells, human T cells express TLR5, allowing CAR(Fla)-T cells to improve their activities via autocrine Fla. Furthermore, TLR5 also expresses on a variety of tumor cells, and TLR5 activation, particularly by Fla, can significantly decrease tumor cell growth.<sup>9 42 43</sup> Although we did not observe this direct antitumor activity of Fla because we chose TLR5-negative tumor cells to better evaluate the contribution of tumor-infiltrating immune cells, these studies, combined with our findings, suggest that our strategy of Fla delivery by CAR-T cells has a high application potential in humans, particularly in patients with TLR5<sup>+</sup> tumors.

In summary, we have demonstrated that delivering Fla into tumors via CAR-T cells can remodel the TME

by converting M2 macrophages into M1 phenotype. This not only enhances the therapeutic effects of CAR-T cells in solid tumors but also promotes endogenous antitumor response mediated by CD8<sup>+</sup> T cells, offering better control of tumors with high antigen heterogeneity. This study introduces a novel strategy to incorporate an additional immune-stimulating pathway into engineered tumor-specific T cells, thereby improving their efficacy. This approach has significant translational potential, as it could be applied to a wide range of solid tumors, given that almost all tumor progression is linked to abnormal macrophage polarization within TME.

**Contributors** GZ and XN conceived the project and designed the experiments. XN, PZ, LD, XP, ZL and YT performed the experiments and acquired the data. XN wrote the first draft of the manuscript. GZ revised the manuscript. XW supervised the entire work. All authors read and approved the final manuscript. XW and GZ are responsible for the overall content as the guarantor.

**Funding** This study was supported by the National Key R&D Program of China (2019YFA0906100), National Natural Science Foundation of China (NSFC, 82471765), Guangdong Basic and Applied Basic Research Foundation (2023A1515030028), Shenzhen Science and Technology Program (JCYJ20220818100806015).

**Competing interests** No, there are no competing interests.

**Patient consent for publication** Not applicable.

**Ethics approval** Not applicable.

**Provenance and peer review** Not commissioned; externally peer reviewed.

**Data availability statement** Data are available upon reasonable request. The data underlying this article will be shared on reasonable request to the corresponding author.

**Supplemental material** This content has been supplied by the author(s). It has not been vetted by BMJ Publishing Group Limited (BMJ) and may not have been peer-reviewed. Any opinions or recommendations discussed are solely those of the author(s) and are not endorsed by BMJ. BMJ disclaims all liability and responsibility arising from any reliance placed on the content. Where the content includes any translated material, BMJ does not warrant the accuracy and reliability of the translations (including but not limited to local regulations, clinical guidelines, terminology, drug names and drug dosages), and is not responsible for any error and/or omissions arising from translation and adaptation or otherwise.

**Open access** This is an open access article distributed in accordance with the Creative Commons Attribution Non Commercial (CC BY-NC 4.0) license, which permits others to distribute, remix, adapt, build upon this work non-commercially, and license their derivative works on different terms, provided the original work is properly cited, appropriate credit is given, any changes made indicated, and the use is non-commercial. See <http://creativecommons.org/licenses/by-nc/4.0/>.

## ORCID iDs

Xiangyun Niu <http://orcid.org/0000-0002-0092-0080>

Guizhong Zhang <http://orcid.org/0000-0001-8930-5262>

## REFERENCES

- Labanieh L, Mackall CL. CAR immune cells: design principles, resistance and the next generation. *Nature New Biol* 2023;614:635–48.
- Rafiq S, Hackett CS, Brentjens RJ. Engineering strategies to overcome the current roadblocks in CAR T cell therapy. *Nat Rev Clin Oncol* 2020;17:147–67.
- Sterner RC, Sterner RM. CAR-T cell therapy: current limitations and potential strategies. *Blood Cancer J* 2021;11:69.
- Yeku OO, Purdon TJ, Koneru M, et al. Armored CAR T cells enhance antitumor efficacy and overcome the tumor microenvironment. *Sci Rep* 2017;7:10541.
- Krenciute G, Prinzing BL, Yi Z, et al. Transgenic Expression of IL15 Improves Antiglioma Activity of IL13Rα2-CAR T Cells but Results in Antigen Loss Variants. *Cancer Immunol Res* 2017;5:571–81.
- Hu B, Ren J, Luo Y, et al. Augmentation of Antitumor Immunity by Human and Mouse CAR T Cells Secreting IL-18. *Cell Rep* 2017;20:3025–33.
- Schnare M, Barton GM, Holt AC, et al. Toll-like receptors control activation of adaptive immune responses. *Nat Immunol* 2001;2:947–50.
- Liu G, Tarbet B, Song L, et al. Immunogenicity and efficacy of flagellin-fused vaccine candidates targeting 2009 pandemic H1N1 influenza in mice. *PLoS ONE* 2011;6:e20928.
- Hajam IA, Dar PA, Shahnawaz I, et al. Bacterial flagellin-a potent immunomodulatory agent. *Exp Mol Med* 2017;49:e373.
- Taylor DN, Treanor JJ, Strout C, et al. Induction of a potent immune response in the elderly using the TLR-5 agonist, flagellin, with a recombinant hemagglutinin influenza-flagellin fusion vaccine (VAX125, STF2.HA1 SI). *Vaccine (Auckl)* 2011;29:4897–902.
- Cai Z, Sanchez A, Shi Z, et al. Activation of Toll-like receptor 5 on breast cancer cells by flagellin suppresses cell proliferation and tumor growth. *Cancer Res* 2011;71:2466–75.
- Sfondrini L, Rossini A, Besusso D, et al. Antitumor activity of the TLR-5 ligand flagellin in mouse models of cancer. *J Immunol* 2006;176:6624–30.
- Brackett CM, Kojouharov B, Veith J, et al. Toll-like receptor-5 agonist, entolimod, suppresses metastasis and induces immunity by stimulating an NK-dendritic-CD8+ T-cell axis. *Proc Natl Acad Sci U S A* 2016;113:E874–83.
- Kaczanowska S, Davila E. Ameliorating the tumor microenvironment for antitumor responses through TLR5 ligand-secreting T cells. *Oncoimmunology* 2016;5:e1076609.
- Roybal KT, Williams JZ, Morsut L, et al. Engineering T Cells with Customized Therapeutic Response Programs Using Synthetic Notch Receptors. *Cell* 2016;167:419–32.
- Kochenderfer JN, Yu Z, Frasher D, et al. Adoptive transfer of syngeneic T cells transduced with a chimeric antigen receptor that recognizes murine CD19 can eradicate lymphoma and normal B cells. *Blood* 2010;116:3875–86.
- Kochenderfer JN, Feldman SA, Zhao Y, et al. Construction and preclinical evaluation of an anti-CD19 chimeric antigen receptor. *J Immunother* 2009;32:689–702.
- Milone MC, Fish JD, Carpenito C, et al. Chimeric receptors containing CD137 signal transduction domains mediate enhanced survival of T cells and increased antileukemic efficacy in vivo. *Mol Ther* 2009;17:1453–64.
- Kutner RH, Zhang XY, Reiser J. Production, concentration and titration of pseudotyped HIV-1-based lentiviral vectors. *Nat Protoc* 2009;4:495–505.
- Long AH, Haso WM, Shern JF, et al. 4-1BB costimulation ameliorates T cell exhaustion induced by tonic signaling of chimeric antigen receptors. *Nat Med* 2015;21:581–90.
- Lee SE, Kim SY, Jeong BC, et al. A bacterial flagellin, *Vibrio vulnificus* FlaB, has a strong mucosal adjuvant activity to induce protective immunity. *Infect Immun* 2006;74:694–702.
- Newick K, O'Brien S, Moon E, et al. CAR T Cell Therapy for Solid Tumors. *Annu Rev Med* 2017;68:139–52.
- Albert ML, Sauter B, Bhardwaj N. Dendritic cells acquire antigen from apoptotic cells and induce class I-restricted CTLs. *Nature New Biol* 1998;392:86–9.
- Jin C, Ma J, Ramachandran M, et al. CAR T cells expressing a bacterial virulence factor trigger potent bystander antitumor responses in solid cancers. *Nat Biomed Eng* 2022;6:830–41.
- Biswas SK, Gangi L, Paul S, et al. A distinct and unique transcriptional program expressed by tumor-associated macrophages (defective NF-κappaB and enhanced IRF-3/STAT1 activation). *Blood* 2006;107:2112–22.
- Murray PJ. Macrophage Polarization. *Annu Rev Physiol* 2017;79:541–66.
- Crellin NK, Garcia RV, Hadisfar O, et al. Human CD4+ T cells express TLR5 and its ligand flagellin enhances the suppressive capacity and expression of FOXP3 in CD4+CD25+ T regulatory cells. *J Immunol* 2005;175:8051–9.
- Hossain MS, Ramachandran S, Gewirtz AT, et al. Recombinant TLR5 agonist CBLB502 promotes NK cell-mediated anti-CMV immunity in mice. *PLoS ONE* 2014;9:e96165.
- Hou AJ, Chang ZL, Lorenzini MH, et al. TGF-β-responsive CAR-T cells promote anti-tumor immune function. *Bioeng Transl Med* 2018;3:75–86.
- Kloss CC, Lee J, Zhang A, et al. Dominant-Negative TGF-β Receptor Enhances PSMA-Targeted Human CAR T Cell Proliferation And Augments Prostate Cancer Eradication. *Mol Ther* 2018;26:1855–66.
- Stromnes IM, Burrack AL, Hulbert A, et al. Differential Effects of Depleting versus Programming Tumor-Associated Macrophages on



- Engineered T Cells in Pancreatic Ductal Adenocarcinoma. *Cancer Immunol Res* 2019;7:977–89.
- 32 Parihar R, Rivas C, Huynh M, *et al.* NK Cells Expressing a Chimeric Activating Receptor Eliminate MDSCs and Rescue Impaired CAR-T Cell Activity against Solid Tumors. *Cancer Immunol Res* 2019;7:363–75.
  - 33 Parisi G, Saco JD, Salazar FB, *et al.* Persistence of adoptively transferred T cells with a kinetically engineered IL-2 receptor agonist. *Nat Commun* 2020;11:660.
  - 34 Pituch KC, Miska J, Krenciute G, *et al.* Adoptive Transfer of IL13Rα2-Specific Chimeric Antigen Receptor T Cells Creates a Pro-inflammatory Environment in Glioblastoma. *Mol Ther* 2018;26:986–95.
  - 35 Ma L, Hostetler A, Morgan DM, *et al.* Vaccine-boosted CAR T crosstalk with host immunity to reject tumors with antigen heterogeneity. *Cell* 2023;186:3148–65.
  - 36 Evans LDB, Hughes C, Fraser GM. Building a flagellum outside the bacterial cell. *Trends Microbiol* 2014;22:566–72.
  - 37 Murthy KGK, Deb A, Goonesekera S, *et al.* Identification of conserved domains in Salmonella muenchen flagellin that are essential for its ability to activate TLR5 and to induce an inflammatory response in vitro. *J Biol Chem* 2004;279:5667–75.
  - 38 Burdelya LG, Krivokrysenko VI, Tallant TC, *et al.* An agonist of toll-like receptor 5 has radioprotective activity in mouse and primate models. *Science* 2008;320:226–30.
  - 39 Solinas G, Germano G, Mantovani A, *et al.* Tumor-associated macrophages (TAM) as major players of the cancer-related inflammation. *J Leukoc Biol* 2009;86:1065–73.
  - 40 Krieg AM. Therapeutic potential of Toll-like receptor 9 activation. *Nat Rev Drug Discov* 2006;5:471–84.
  - 41 Zheng JH, Nguyen VH, Jiang S-N, *et al.* Two-step enhanced cancer immunotherapy with engineered *Salmonella typhimurium* secreting heterologous flagellin. *Sci Transl Med* 2017;9:eaak9537.
  - 42 Schmausser B, Andrulis M, Endrich S, *et al.* Toll-like receptors TLR4, TLR5 and TLR9 on gastric carcinoma cells: an implication for interaction with Helicobacter pylori. *Int J Med Microbiol* 2005;295:179–85.
  - 43 Rhee SH, Im E, Pothoulakis C. Toll-like receptor 5 engagement modulates tumor development and growth in a mouse xenograft model of human colon cancer. *Gastroenterology* 2008;135:518–28.